

KFKI-2000-02/G
REPORT

Z. HÓZER
L. MARÓTI
I. NAGY
P. WINDBERG

**CODEX-2 EXPERIMENT:
INTEGRAL VVER-440 CORE DEGRADATION TEST**

Hungarian Academy of Sciences
CENTRAL
RESEARCH
INSTITUTE FOR
PHYSICS

B U D A P E S T

**CODEX-2 EXPERIMENT:
INTEGRAL VVER-440 CORE DEGRADATION TEST**

Z.Hózer, L. Maróti, I. Nagy, P. Windberg

KFKI Atomic Energy Research Institute
P.O.Box 49,
H-1525 Budapest, Hungary

Contents

1. INTRODUCTION	4
2. THE CODEX FACILITY	5
3. THE EXPERIMENTAL PROGRAMME	8
4. THE CODEX-2 EXPERIMENT	9
5. EXPERIMENTAL RESULTS.....	9
6. CONCLUSIONS	12
ACKNOWLEDGMENTS.....	12
REFERENCES.....	12

List of tables

TABLE 1 MAIN CHARACTERISTICS OF THE CODEX-2 BUNDLE	5
TABLE 2 PYROMETER CHARACTERISTICS	6
TABLE 3 THERMOCOUPLE (TC) CHARACTERISTICS	7
TABLE 4 TEMPERATURE MEASUREMENTS	7
TABLE 5 MEASUREMENTS OF SYSTEM PARAMETERS	8
TABLE 6 MAIN PARAMETERS OF CODEX TEST MATRIX	8
TABLE 7 LIST OF PARAMETERS AVAILABLE IN THE CODEX-2 EXPERIMENTAL DATABASE	10

List of figures

FIG. 1 SCHEME OF THE CODEX FACILITY	13
FIG. 2 HORIZONTAL CROSS SECTION OF THE CODEX-2 BUNDLE	14
FIG. 3 ELECTRICAL RESISTANCE OF THE W HEATER AS FUNCTION OF TEMPERATURE	14
FIG. 4 LOCATIONS OF THERMOCOUPLES AND PYROMETERS	15
FIG. 5 H CONCENTRATION MEASUREMENT	16
FIG. 6 HEATED ROD OF THE CODEX BUNDLE	17
FIG. 7 UH50: UNHEATED ROD TEMPERATURE AT 50 MM	18
FIG. 8 UH175: UNHEATED ROD TEMPERATURE AT 175 MM	18
FIG. 9 UH300: UNHEATED ROD TEMPERATURE AT 300 MM	19
FIG. 10 UH425: UNHEATED ROD TEMPERATURE AT 425 MM	19
FIG. 11 UH550: UNHEATED ROD TEMPERATURE AT 550 MM	20
FIG. 12 SH50: SHROUD TEMPERATURE AT 50 MM	20
FIG. 13 SH300: SHROUD TEMPERATURE AT 300 MM	21
FIG. 14 SH550: SHROUD TEMPERATURE AT 550 MM	21
FIG. 15 HTS550: STEEL TEMPERATURE AT 550 MM	22
FIG. 16 HI300: EXTERNAL INSULATION TEMPERATURE AT 300 MM	22
FIG. 17 PYR300: PYROMETER TEMPERATURE AT 300 MM	23
FIG. 18 PYR550: PYROMETER TEMPERATURE AT 550 MM	23
FIG. 19 TCIN: COOLANT INLET TEMPERATURE	24
FIG. 20 TCOU: COOLANT OUTLET TEMPERATURE	24
FIG. 21 TSTEAM: STEAM TEMPERATURE IN STEAM GENERATOR	25
FIG. 22 TAMB: AMBIENT TEMPERATURE IN THE CONTAINMENT VESSEL	25
FIG. 23 ARGON: ARGON FLOWRATE	26
FIG. 24 STEAM: STEAM FLOWRATE	26
FIG. 25 H2: HYDROGEN FLOWRATE	27
FIG. 26 LSG: EVAPORATED WATER VOLUME IN STEAM GENERATOR	27
FIG. 27 LCOND: CONDENSED WATER VOLUME	28
FIG. 28 VOLTAGE: VOLTAGE ON THE HEATER RODS	28
FIG. 29 CURRENT: CURRENT ON THE HEATER RODS	29
FIG. 30 POWER: TOTAL ELECTRICAL POWER OF THE HEATER RODS	29
FIG. 31 RESIST: ELECTRICAL RESISTANCE OF THE HEATER RODS	30
FIG. 32 VIEW AND CROSS SECTIONS OF THE CODEX-2 BUNDLE	31
FIG. 33 CODEX-2 BUNDLE CROSS SECTION AT 305 MM ELEVATION	32
FIG. 34 HORIZONTAL CROSS-SECTION OF CODEX-2 BUNDLE AT ELEVATION 390 MM.	33

1. INTRODUCTION

The processes of the early phase of the core melting play important role from both physical and technological points of view. The high temperature results in the interaction of different core materials, such as UO₂ pellets, cladding, spacer, shroud of the assembly and coolant. New chemical compositions are produced. The high temperature leads to the deformation of pellets and cladding and also to the partial melting of fuel assemblies. Due to the mechanical damage and melting of fuel rods broken fragments and debris can fall down and create blockage of the flow channel. These phenomenon needs experimental investigation on integral test facilities with fuel assembly simulators.

As the different nuclear reactors have different geometrical arrangement and include various kinds of materials the experiments must reflect the plant specific characteristics. The CODEX-VVER experimental programme was launched in KFKI Atomic Energy Research Institute in order to investigate core degradation phenomena focusing on the specific features of VVER-440 reactors.

2. THE CODEX FACILITY

The CODEX (COre Degradation EXperiment) integral test facility represents the geometrical arrangement of a VVER-440 reactor fuel assembly and has been constructed of VVER materials. A schematic view of the facility is shown in Fig.1. The basic part of the facility is the test section comprising a seven rod bundle of 600 mm heated length. The rods arranged in hexagonal geometry, the external diameter of the cladding is 9,13 mm. The six peripheral rods are electrically heated by tungsten bars. The central rod is not heated and it includes a bar for thermocouples. The 3,0 mm diameter bars in the heated rods are surrounded with ring-shaped UO_2 pellets - 3,6% enrichment of U^{235} - and enclosed in industrially fabricated Zr1%Nb alloy cladding. Pt covered Mo wires of 1,2 mm external diameter in spiral form are used for the connection of the W bars to the electrodes. Water cooling jacket are used to cool the bottom and the top of the electrodes. The rods are filled up with argon, the internal pressure is 1,2 bar. The diameter of the hole in the pellet equals to 3,3 mm, while the external pellet diameter is 7,57 mm. The bundle is fixed by three spacer grids, which are made of stainless steel. The spacers are located on elevations of 50 mm, 300 mm and 550 mm.

Bundle type	VVER-440
Number of rods	7
Number of heated rods	6
Number of unheated rods	1
Pitch size	12,2 mm
Cladding external diameter	9,13 mm
Cladding internal diameter	7,72 mm
Cladding material	Zr1%Nb
Heater material	W
Heater bar diameter	3 mm
Pellets in heated rods	UO_2
External diameter of UO_2 pellets	7,57 mm
Internal diameter of UO_2 pellets	3,3 mm
Height of pellets	10-13 mm
Heated length with UO_2 pellets	600 mm
UO_2 enrichment	3,6%
Pellets in unheated rod	none
Material of spacer grids	stainless steel 06X18H10T
Number of spacer grids	3
Positions of spacer grids	50 mm, 300 mm, 550 mm
Height of spacer grids	10 mm
Shroud material	Zr2%Nb
Shroud thickness	2 mm
Internal key size of shroud	35,9 mm
Length of shroud	600 mm

Table 1 Main characteristics of the CODEX-2 bundle

The bundle is placed into a hexagonal shroud. The shroud material is Zr2.5%Nb alloy, the same alloy is used for the canisters in the real power plant assemblies. The shroud has no

perforations. The relatively large mass of shroud alloy can result in high hydrogen production. This shroud is surrounded by several thermal insulation layers of ZrO_2 (13 mm thickness), Al_2O_3 (92 mm external diameter), stainless steel (98 mm and 106 mm internal and external diameters) and mineral cotton (200 mm thickness). Between Al_2O_3 and stainless steel layers a small air gap is kept to compensate thermal expansion. The cross section of bundle is given in Fig. 2 and the correlation for the calculation of the electrical resistance of the W heaters in Fig. 3.

The test section has inlet and outlet junctions for the coolant at 0 and 650 mm elevations respectively. Two observation windows makes possible the temperature measurements at 300 and 550 mm elevations by pyrometers.

The steam generator and superheater section of the facility provides argon and steam inlet flow for the test section during heating-up and cooling-down phases. The 4 kW superheater and 18 kW steam generator powers produce high coolant temperatures ($\sim 600^\circ C$) for the experiments.

An additional tank can be used for quenching the test section and cooling down the bundle quickly by water. This tank is connected to the lower part of the test section and thus provides a possibility for bottom-up quenching.

The coolant leaving the upper part of the test section flows through a steam condenser and enters the off gas system with filters. The coolant cools down, the steam condenses and the water is collected at the bottom of cooler-condenser unit. The high surface molecule-filters prevent release of aerosol particles, only noncondensable gases are released during the test. The hydrogen concentration is measured in the off-gas system using a palladium valve system. The gas mixture with H content enters a volume, which is kept under depression using vacuum system and capillary tube. A thermal-cross type device placed in this volume measures the thermal conductivity of the gas. The increase of thermal conductivity indicates the increase of H concentration in the coolant, for the Pa valve allows only the H to enter the volume. Before the experiment the H measurement system needed thorough calibration.

The main parameters are collected in the data acquisition system. The values of input voltage and current, coolant flow rate, coolant inlet and outlet temperatures, condensate level, steam generator level, system pressure, hydrogen concentration and rod temperatures are measured during the test. Several high temperature W-Re thermocouples are built into the rods, shroud, insulation layers at different elevations and special windows for optical pyrometers are mounted in the test section in order to provide information on the course of experiments (Fig. 4.).

Pyrometer	1.	2.
type	integral radiation measurement	proportional, two-color radiation measurement
position	upper space grid	central spacer grid

Table 2 Pyrometer characteristics

TC	1. (W1)	2. (W2)	3. (Pt)	4. (Ni)
type	WR5%Re- W26%Re	W5%Re- W20%Re	Pt-Pt13%Rh	NiCr-NiAl
insulation	BeO	HfO ₂	Al ₂ O ₃	MgO ₂
shroud	tantalum, niobium	niobium	platinum	stainless steel
external diameter	2.3 mm	2.3 mm	1.5 mm	0.8 mm

Table 3 Thermocouple (TC) characteristics

Temperature measurement	TC material/type	Position [mm]	Placement
UH50	Pt	50	central unheated rod
UH175	W2	175	central unheated rod
UH300	W2	300	central unheated rod
UH425	W1	425	central unheated rod
UH550	W1	550	central unheated rod
SH50	Ni	50	shroud
SH300	Pt	300	shroud
SH425	Pt	425	shroud
SH550	Pt	550	shroud
HTS550	Ni	550	high temp. insulation, steel
HI300	Ni	300	high temp. insulation
PYR300	proportional pyrometer	300	bundle/observation window
PYR550	integral pyrometer	550	bundle/observation window
TCIN	Ni	0	coolant inlet junction
TCOUT	Ni	650	coolant outlet junction
TSTEAM	Ni		steam generator
TAMB	Ni		containment vessel

Table 4 Temperature measurements

parameter	device	placement
Argon flowrate	calibrated valve	gas supply system
Steam flowrate	steam generator el. power	steam generator
H ₂ concentration	palladium valve system	gas off system
Steam generator level	DP transducer, 20 mbar/4-20 mA	steam generator
Condensate water level	DP transducer ,60 mbar/4-20 mA	condensate tank
Voltage	shunt	rail of power supply
Current	el. power	rail of power supply
Gas pressure in rods	P transducer, 2.5 bar/4-20 mA	fuel rods

Table 5 Measurements of system parameters

3. THE EXPERIMENTAL PROGRAMME

In AEKI an experimental programme was initiated focusing on the high temperature behaviour of VVER fuel and core materials. The interactions of Zr1%Nb cladding with UO₂ pellet, stainless steel spacer and boron steel absorber were studied in small scale separate effect tests. [1][2] On the basis of the experience gained in these tests the CODEX integral test facility was constructed to continue this work under more prototypic conditions.

The VVER experimental programme consisted of four tests. The main parameters of the test matrix are given in Table 2.

Test	Bundle type	Pellet	Year	Test type
CODEX-1	7-rod VVER	Al ₂ O ₃	1995	scoping test
CODEX-2	7-rod VVER	UO ₂	1995	escalation and slow cooling down
CODEX-3/1	7-rod VVER	UO ₂	1996	water quench at 1150 °C
CODEX-3/2	7-rod VVER	UO ₂	1997	water quench at 1500 °C

Table 6 Main parameters of CODEX test matrix

First the capabilities of the facility were demonstrated carrying out the CODEX-1 experiment with Al₂O₃ pellets. The test section was heated up with argon, then the electric power was increased. When the rod bundle degradation was indicated by temperature measurements the power was switched off and the section was cooled down by argon. The post-test examination showed that the rod bundle partially damaged, the further melting was stopped in time. So the facility proved to be applicable to the experimental analysis of controlled core degradation processes.

In the second experiment similar procedures were taken, but the Al_2O_3 pellets were replaced with UO_2 [3]. This test is described in the present report.

The CODEX-3/1 and CODEX-3/2 experiments were performed with quick water cooling [4].

4. THE CODEX-2 EXPERIMENT

The first experiment with UO_2 pellets - named CODEX-2 - was performed on 29th December 1995. The experiment consisted of three main phases.

Phase 1. During the first phase of the experiment the bundle was preheated up to $500\text{ }^\circ\text{C}$ by a constant inlet flow of argon (1.4 g/s) with an inlet temperature equal to $600\text{ }^\circ\text{C}$. There was no electrical heating on fuel rods. The stable temperature distribution was established at 9000 s .

Phase 2. The second phase started with switching on electrical rod heating. The electrical power was linearly increased (Fig. 30) with a speed of 2 W/s and steam (Fig. 24) was added to the argon flow (Fig. 23). The argon flow was the same as in the first phase. The steam flow rate was $\sim 1.0\text{ g/s}$ and its temperature $\sim 600\text{ }^\circ\text{C}$ (Fig. 19). When the clad temperature reached $1500\text{ }^\circ\text{C}$ at about 1200 s after the beginning of the second phase a rod temperature escalation was observed (Fig. 10-11). The second phase lasted 1800 s .

Phase 3. In the final phase the cooling down was initiated. The electrical heating was switched off (Fig. 30), the steam injection (Fig. 24) was stopped and the facility was cooled down slowly (in three hours) in argon.

5. EXPERIMENTAL RESULTS

The test phase is related to Phase 2. of the CODEX-2 experiment. The hydrogen concentration started to increase at 500 s after the beginning of Phase 2. The measured hydrogen concentration is shown in Fig. 25, the maximum value (36 mg/s) was reached at 2000 s . The total hydrogen production during this test was 26.6 g . The presence of hydrogen indicates the chemical reaction between cladding and steam. This reaction contributed to the heat up and was the cause of the escalation of rod temperatures. The pyrometer measurements showed that the highest temperature - $2400\text{ }^\circ\text{C}$ - was reached close to the top of the bundle (Fig. 18). In the lower part of the bundle - 50 mm from the bottom of the heated zone - the maximum temperature remained below $750\text{ }^\circ\text{C}$ (Fig. 7). Large temperature differences were found between rods and shroud. In the upper part of the section - 550 mm from the bottom - the shroud temperature (Fig. 14) was not higher than $1600\text{ }^\circ\text{C}$, while on the same elevation the rod temperature (Fig. 11) reached $2000\text{ }^\circ\text{C}$. The temperature measurements taken by the pyrometers and thermocouples in the central rod and shroud are shown in Fig. 7-18. The steep temperature increase close to 2000 s is the temperature escalation, which indicates the heat up rate due to the clad oxidation runaway.

The experimental data were collected for code validation purposes into a database, which covers 3600 s of the test phase and the cooldown phase with 1 s frequency. The parameters are listed in Table 7 and the plotted in Fig. 7-31.

Name	Definition	Unit
UH50	unheated rod temperature at 50 mm	°C
UH175	unheated rod temperature at 175 mm	°C
UH300:	unheated rod temperature at 300 mm	°C
UH425	unheated rod temperature at 425 mm	°C
UH550	unheated rod temperature at 550 mm	°C
SH50	shroud temperature at 50 mm	°C
SH300	shroud temperature at 300 mm	°C
SH550	shroud temperature at 50 mm	°C
HTS550	steel temperature at 50 mm	°C
HI300	external insulation temperature at 300 mm	°C
PYR300	pyrometer temperature at 300 mm	°C
PYR550	pyrometer temperature at 550 mm	°C
TCIN	coolant inlet temperature	°C
TCOUT	coolant outlet temperature	°C
TSTEAM	steam temperature in steam generator	°C
TAMB	ambient temperature in the containment vessel	°C
ARGON	argon flowrate	g/s
STEAM	steam flowrate	g/s
H2	hydrogen flowrate	mg/s
LSG	evaporated water volume in steam generator	l
LCOND	condensed water volume	l
VOLTAGE	voltage on the heater rods	V
CURRENT	current on the heater rods	A
POWER	total electrical power of the heater rods	W
RESIST	electrical resistance of the heater rods	ohm

Table 7 List of parameters available in the CODEX-2 experimental database

For post test examination of the rods, the bundle was filled up with epoxy and afterwards cut into slices in order to facilitate the further investigation. The visual analysis of the polished cross sections showed that during this experiment the early phase of core degradation was reached : the upper part of the bundle melted down, the lower part had no damage and in the central part the stages of partial loss of geometry were observed. The physical picture of the damaged bundle was found to be consistent with the temperature measurements. The layout of the bundle before filling up with epoxy and five slices of the filled up section are shown in Fig. 32.

In the photograph of the bundle it can be seen, that the shroud and large part of the cladding materials were lost between 400-550 mm elevations. Some part of these materials were melted, but other broken parts fell down and were found as heavily oxidised fragments in the lower part of the section. The cross section at 305 mm (Fig. 33) corresponds to the elevation of spacer grid. The maximum temperature at this point was 1300 °C. Some signs of cladding-spacer interaction were observed and the mechanical break-up of some fuel pellets

can be seen. At lower elevations no serious damage can be observed. Partial damage of the bundle can be seen at 390 mm (Fig. 34). Some fuel claddings were broken, part of the pellets left the rod due to fuel fragments relocation. The gap between pellets and cladding in some rods disappeared and the pellet cladding interaction took place. At 450 mm level the total mechanical break-up of the bundle can be seen (Fig. 32).

The cross section at 390mm elevation is shown in Fig. 34 with the corresponding micro-analytical photographs. The detailed post-test examination of this slice pointed out the melting of Zr (central rod), the phase transition and the different stages of clad oxidation (see the heated rods and the shroud). The oxide layer thickness was also measured. It was found that the average thickness of oxide layer on rods was 180-200 μm , while on the shroud 300 μm and 210 μm on the inner and outer surfaces respectively.

6. CONCLUSIONS

The early phase of core degradation phenomena were experimentally studied on the CODEX test facility using a VVER-440 type electrically heated 7-rod bundle. Conditions were established for the partial core damage, and the further core melting was stopped by the final cooling down procedure.

The new data extends the current database for code validation of VVER-440 severe accident transients and provide information for the extension of western severe accident code capabilities toward VVER applications.

The use of VVER materials and fuel assembly geometry made possible to compare the behaviour of VVER reactors under core damage conditions to the better investigated western type reactors. On the basis of comparisons [3][5] between CODEX-2 and CORA tests it was concluded that during the early phase of core degradation the same phenomena can be expected with VVER materials as with western design reactors. However for numerical simulation VVER specific material properties and correlations must be used.

ACKNOWLEDGMENTS

The CODEX VVER experiments were supported by the National Committee for Technological Development (OMFB) of Hungary.

REFERENCES

- [1] L. Maróti, "VVER Fuel under Extreme Conditions", Transactions of TOPFUEL '95, vol. 1., 1995, pp. 253-264
- [2] L. Maróti, "Chemical Interaction between VVER Core Components under Accidental Conditions", Nucl. Eng. and Design vol. 172, 1997, pp. 73-81
- [3] Z. Hózer, L. Maróti, B. Tóth, P. Windberg, "VVER-440 Core Degradation Experiment" Proceedings of NURETH-8, Vol. 2, Kyoto, 1997, pp. 605-611.
- [4] Z. Hózer, L. Maróti, P. Windberg, "Quenching of High Temperature VVER Bundle", Proceedings of NURETH-9 on CD, San Francisco, 1999, ISBN 0-89448-650-0
- [5] Z. Hózer, K. Trambauer, J. Duspiva, "VVER-Specific Features Regarding Core Degradation", NEA/CSNI/R(98)20, 1998

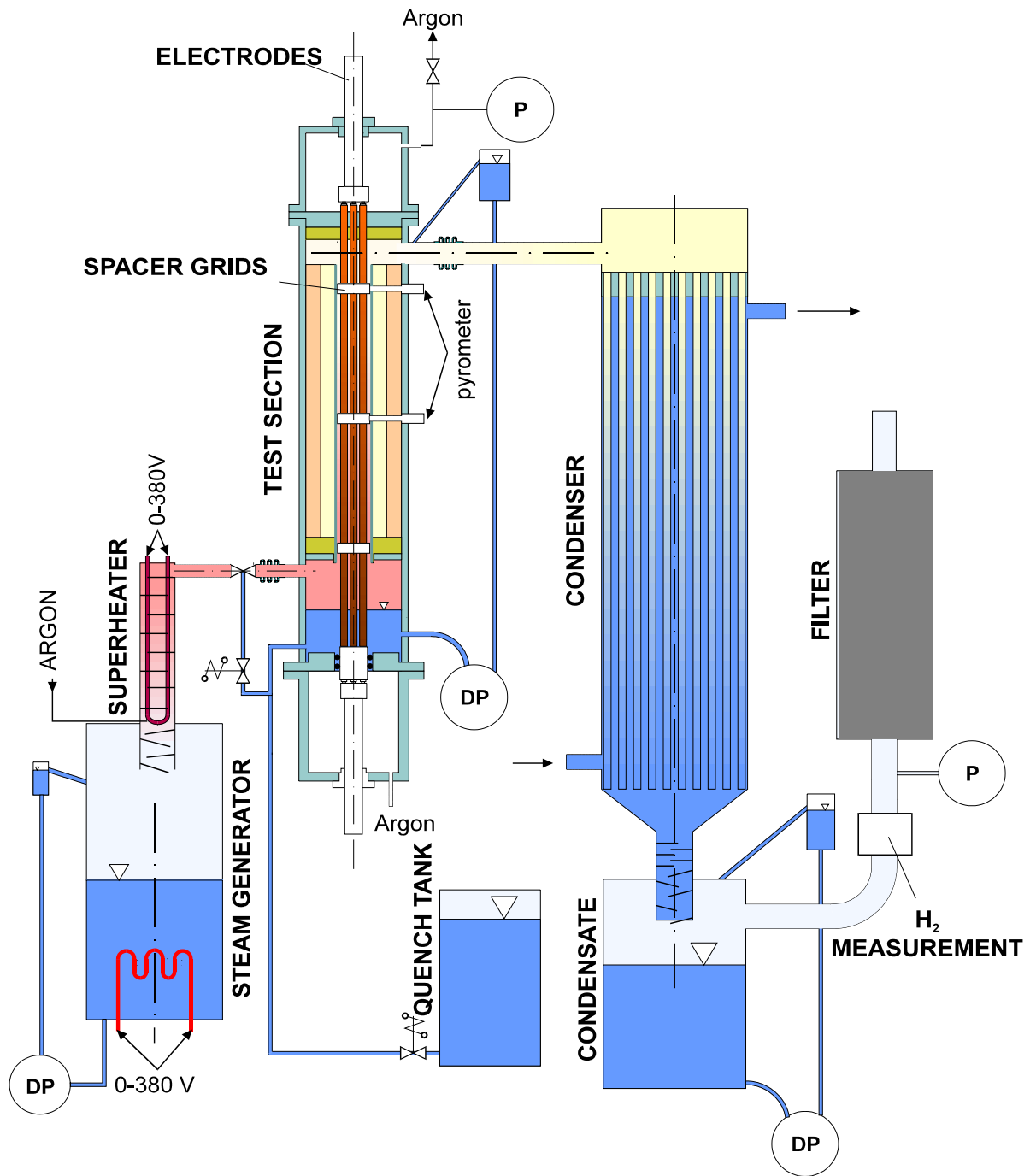


Fig. 1 Scheme of the CODEX facility

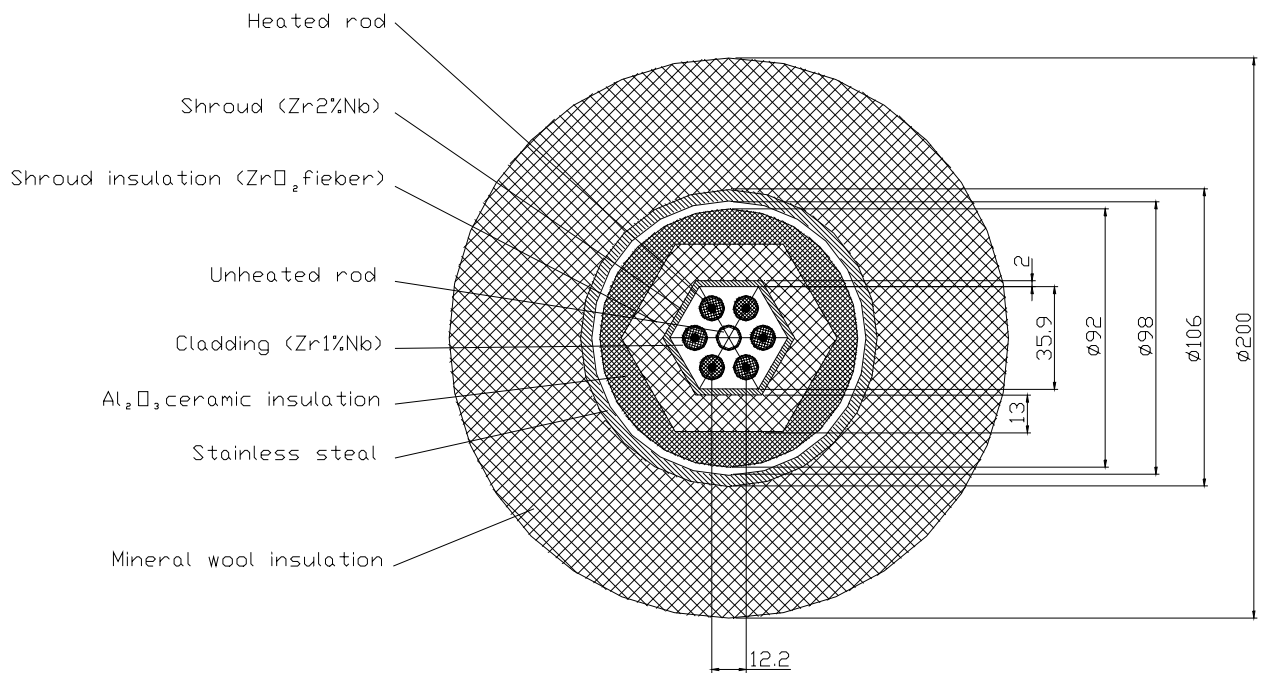


Fig. 2 Horizontal cross section of the CODEX-2 bundle

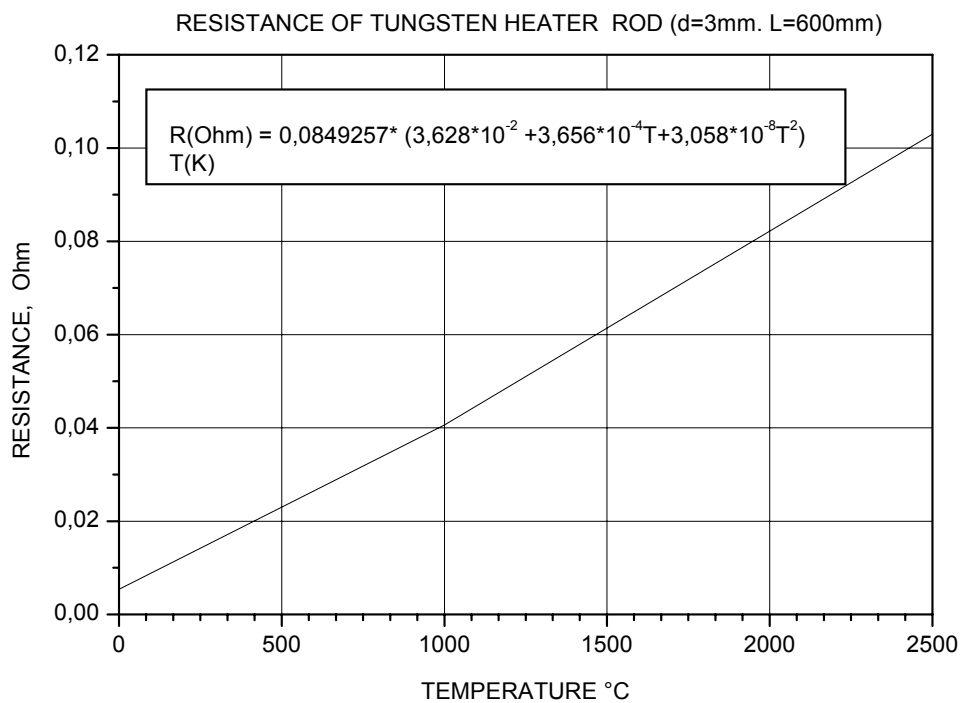


Fig. 3 Electrical resistance of the W heater as function of temperature

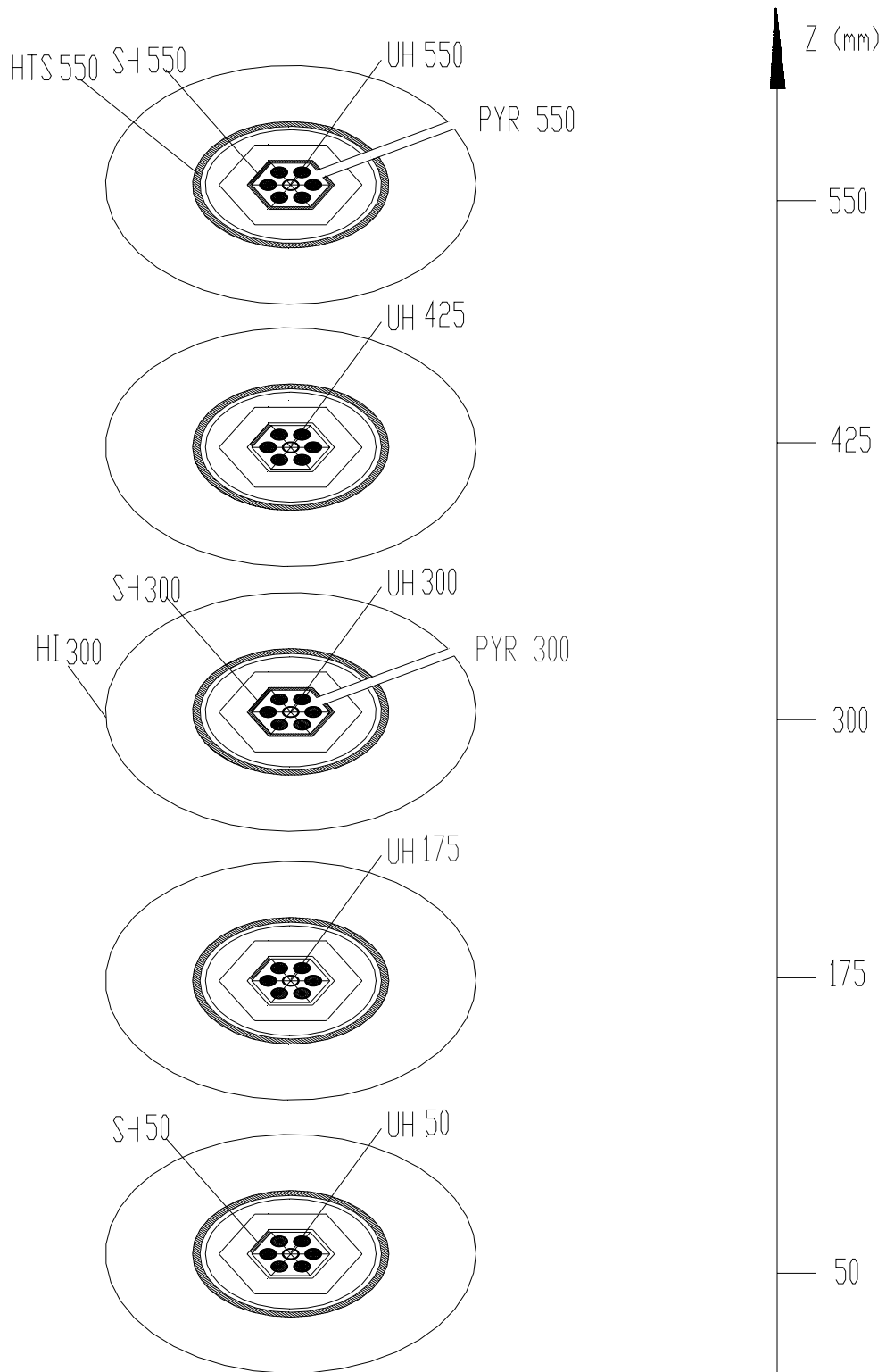


Fig. 4 Locations of thermocouples and pyrometers

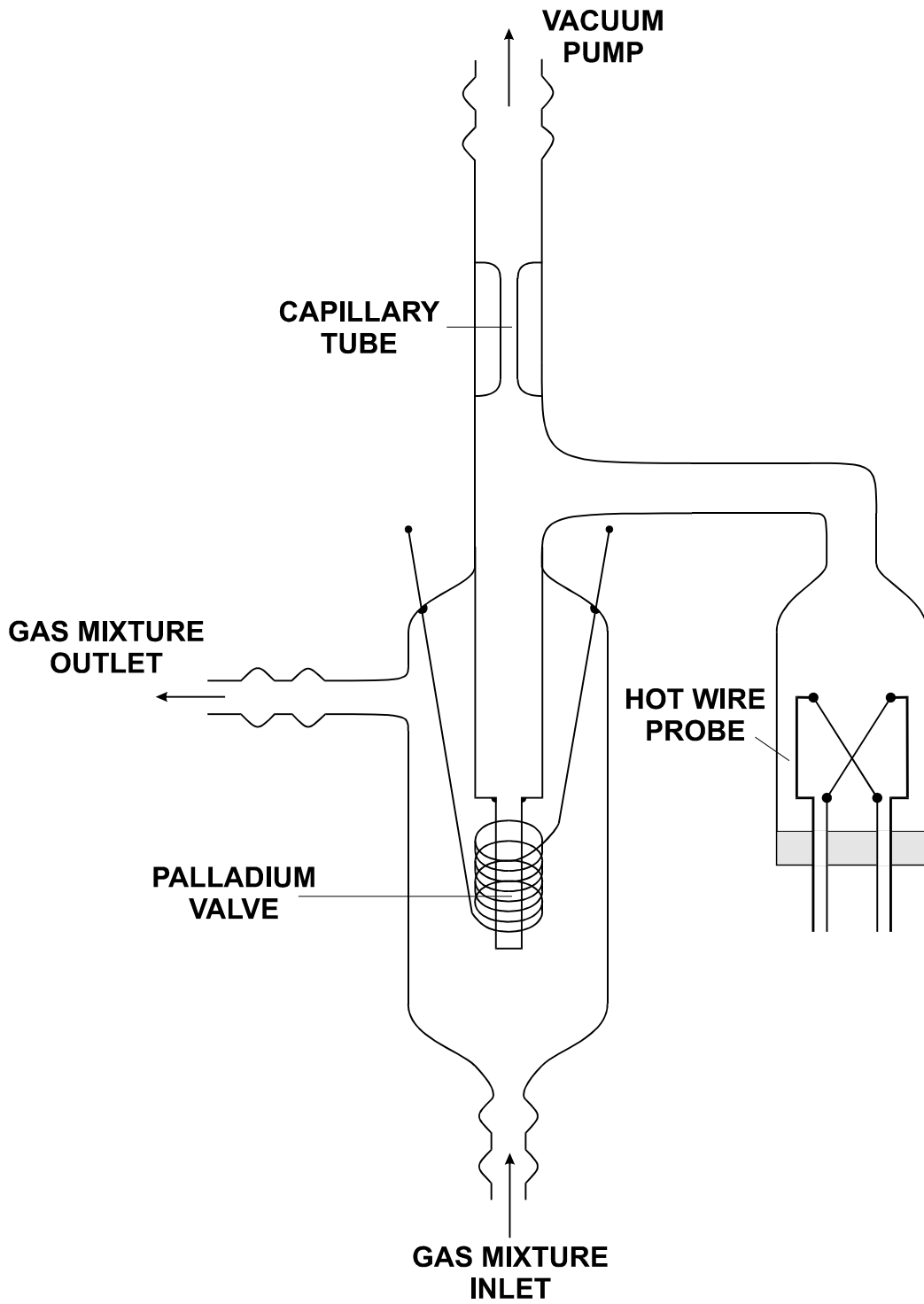


Fig. 5 H concentration measurement

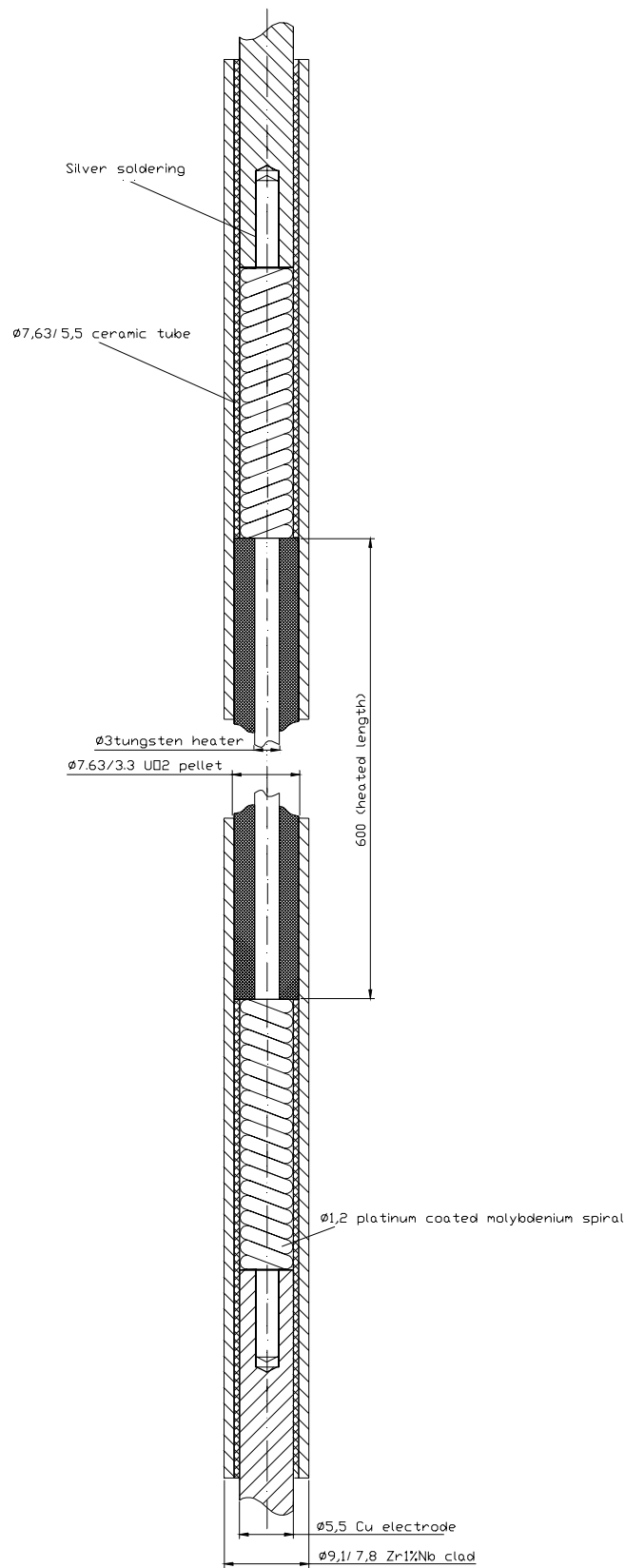


Fig. 6 Heated rod of the CODEX bundle

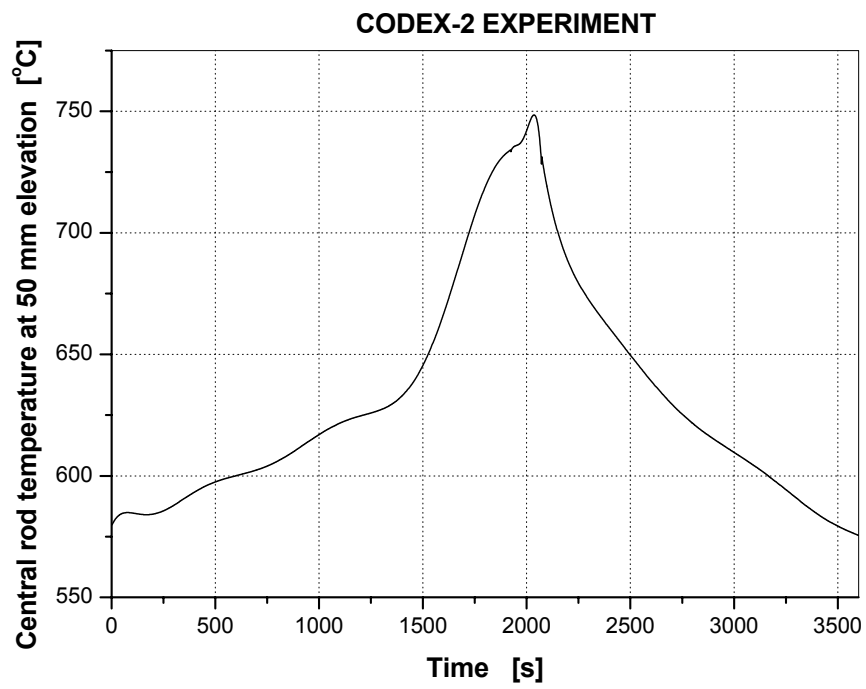


Fig. 7 UH50: unheated rod temperature at 50 mm

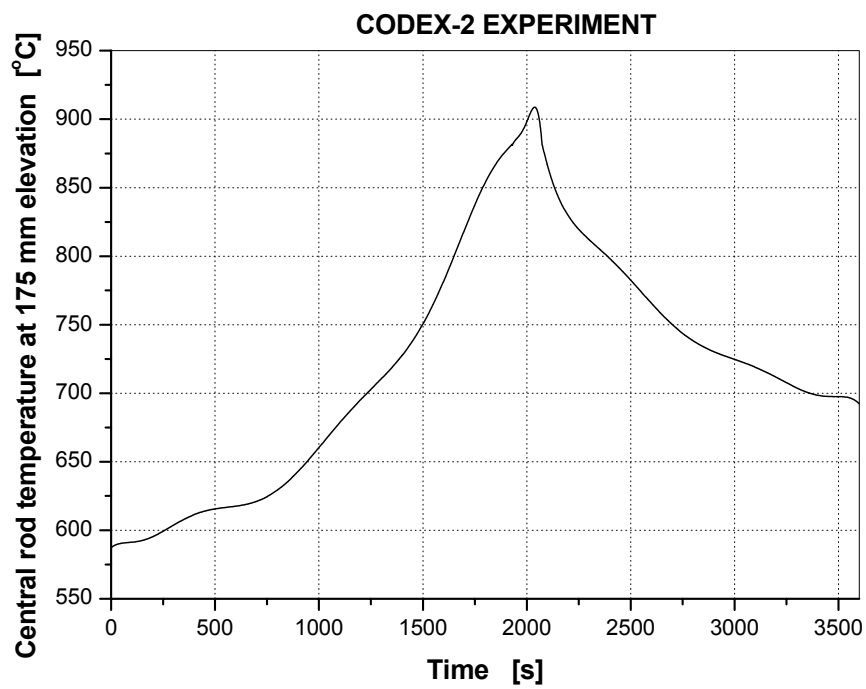


Fig. 8 UH175: unheated rod temperature at 175 mm

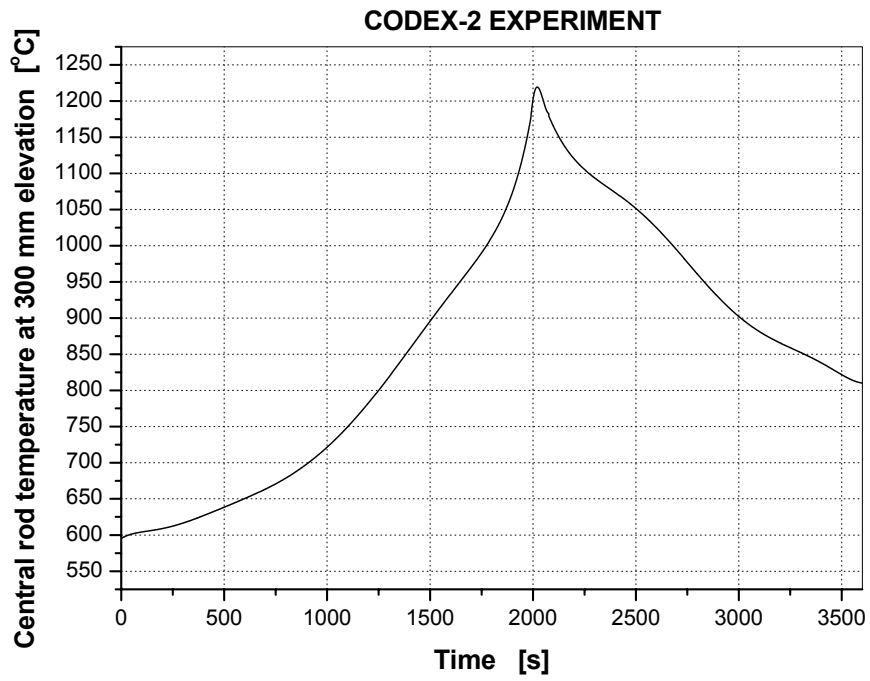


Fig. 9 UH300: unheated rod temperature at 300 mm

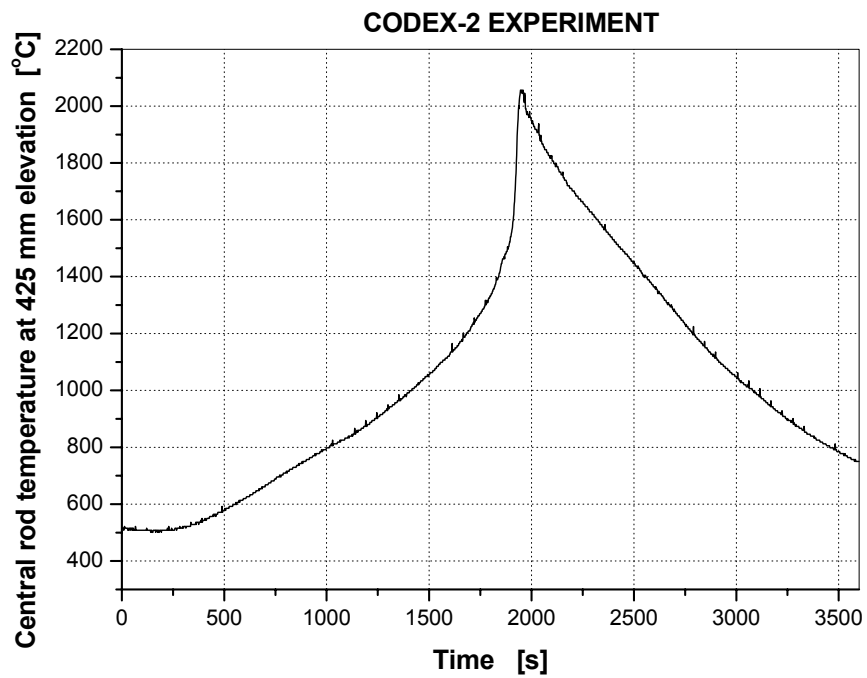


Fig. 10 UH425: unheated rod temperature at 425 mm

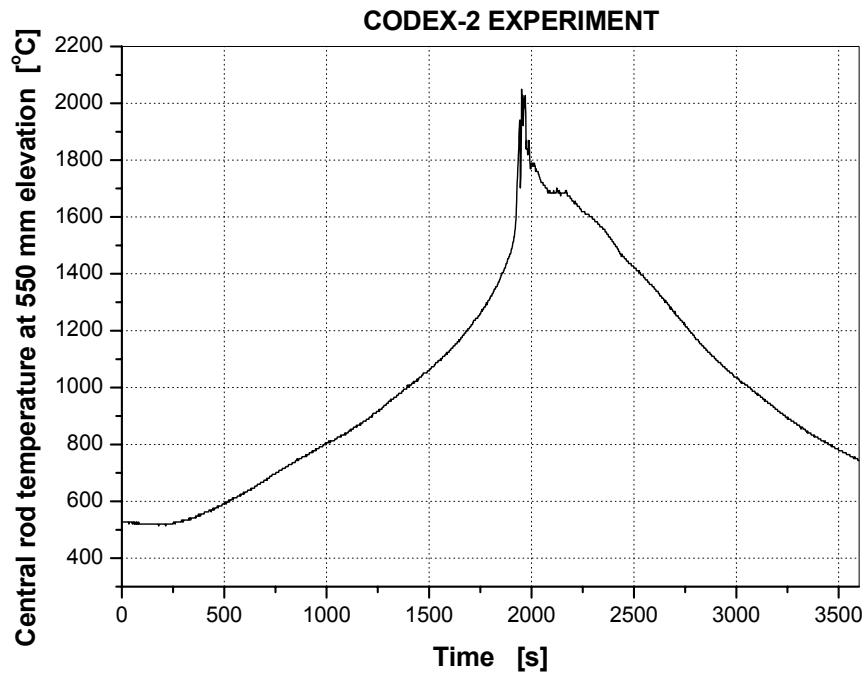


Fig. 11 UH550: unheated rod temperature at 550 mm

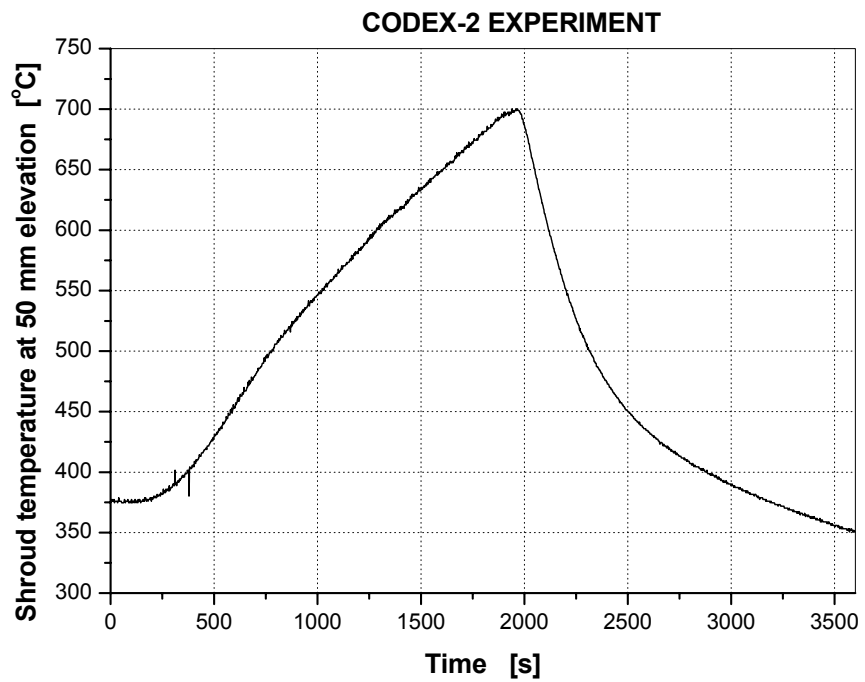


Fig. 12 SH50: shroud temperature at 50 mm

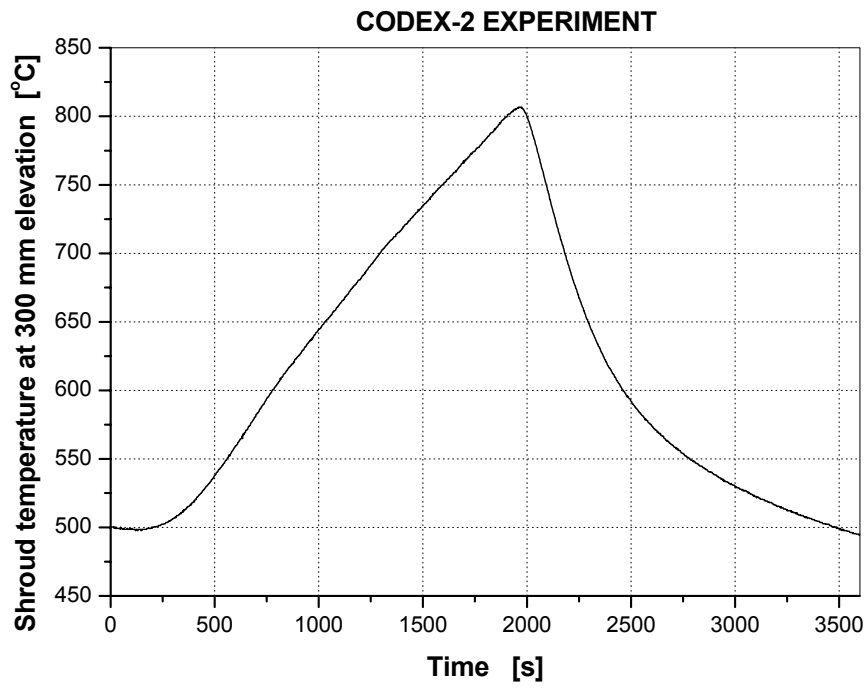


Fig. 13 SH300: shroud temperature at 300 mm

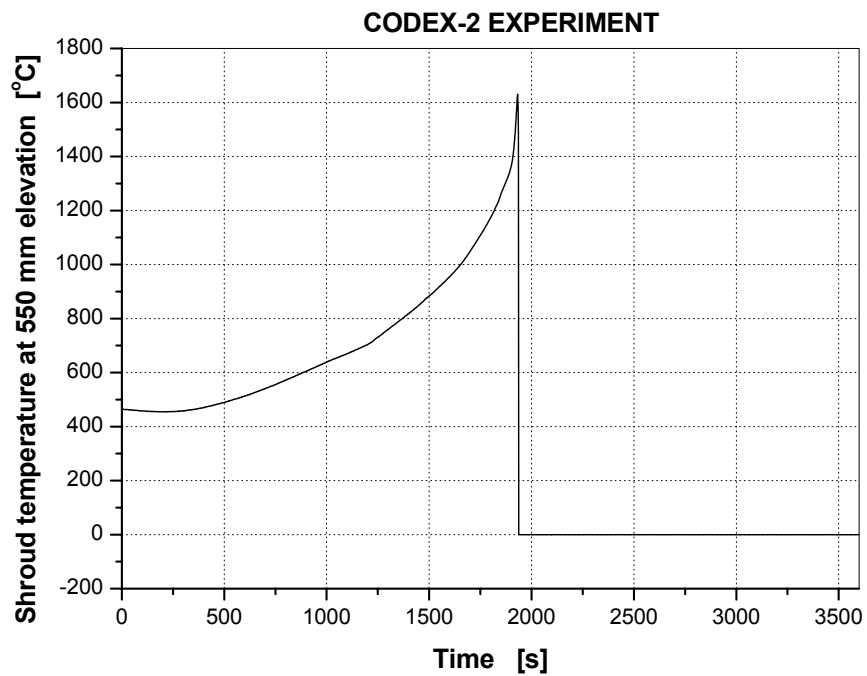


Fig. 14 SH550: shroud temperature at 50 mm

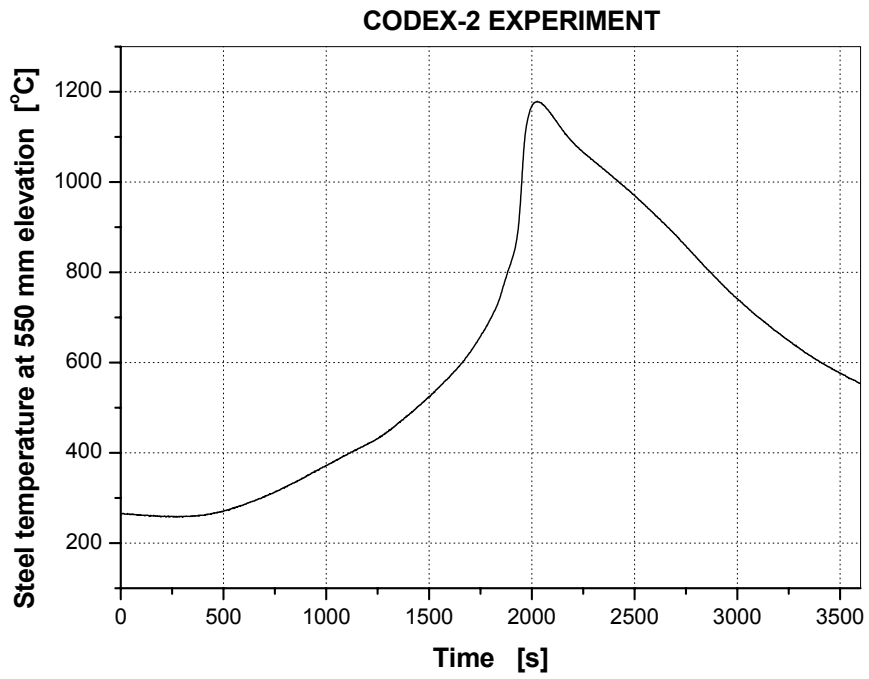


Fig. 15 HTS550: steel temperature at 50 mm

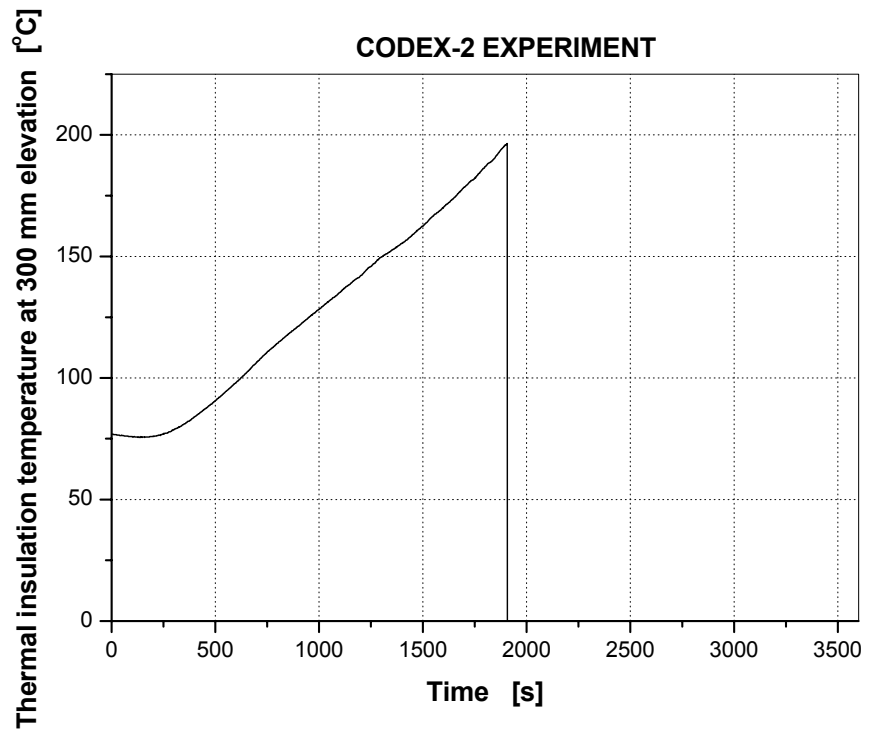


Fig. 16 HI300: external insulation temperature at 300 mm

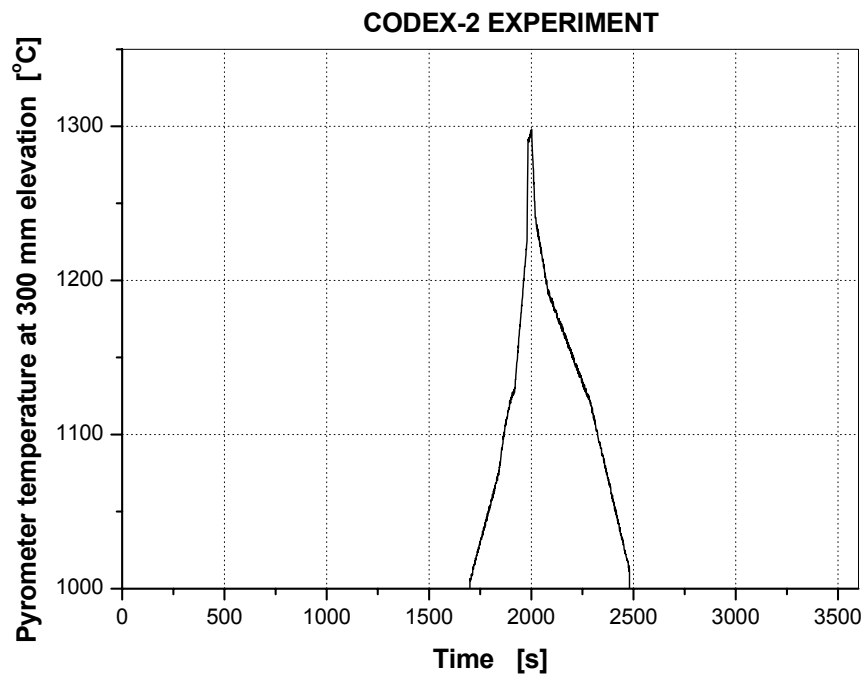


Fig. 17 PYR300: pyrometer temperature at 300 mm

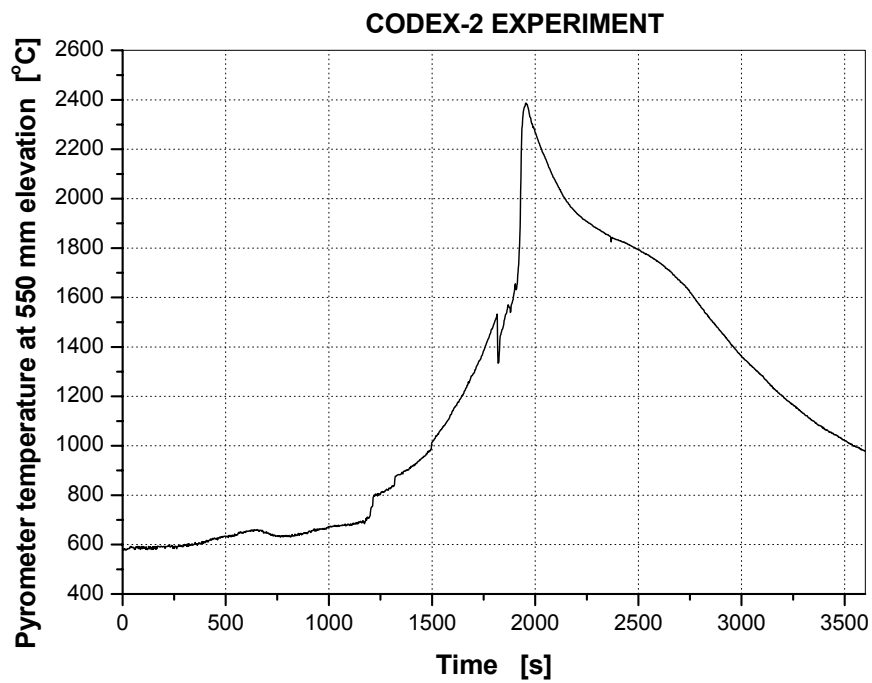


Fig. 18 PYR550: pyrometer temperature at 550 mm

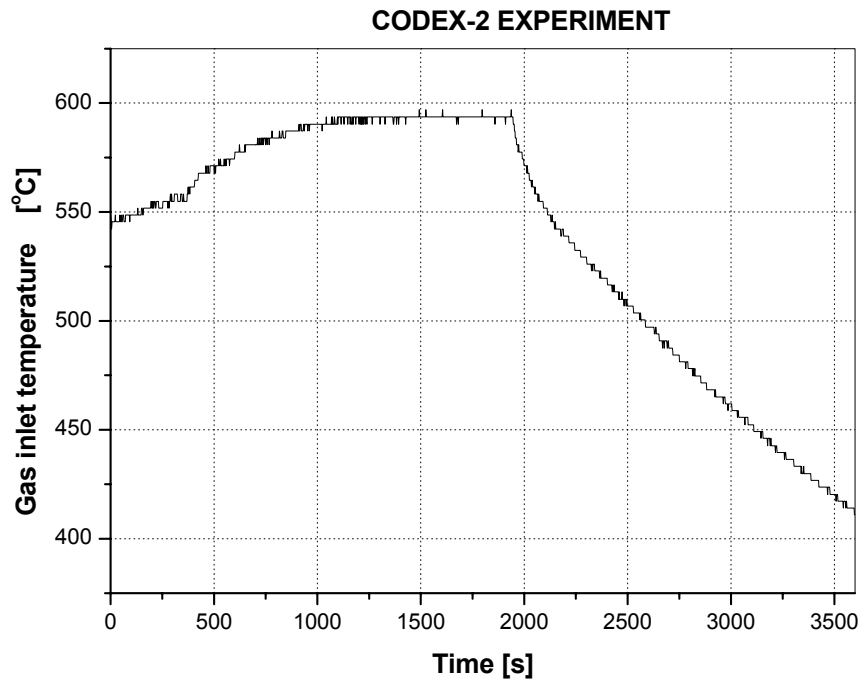


Fig. 19 TCIN: coolant inlet temperature

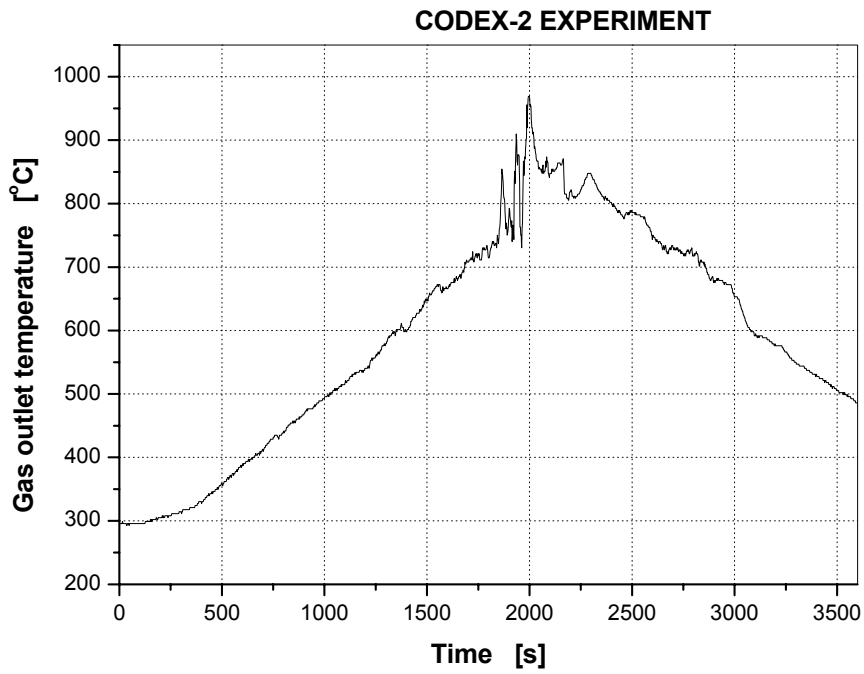


Fig. 20 TCOUT: coolant outlet temperature

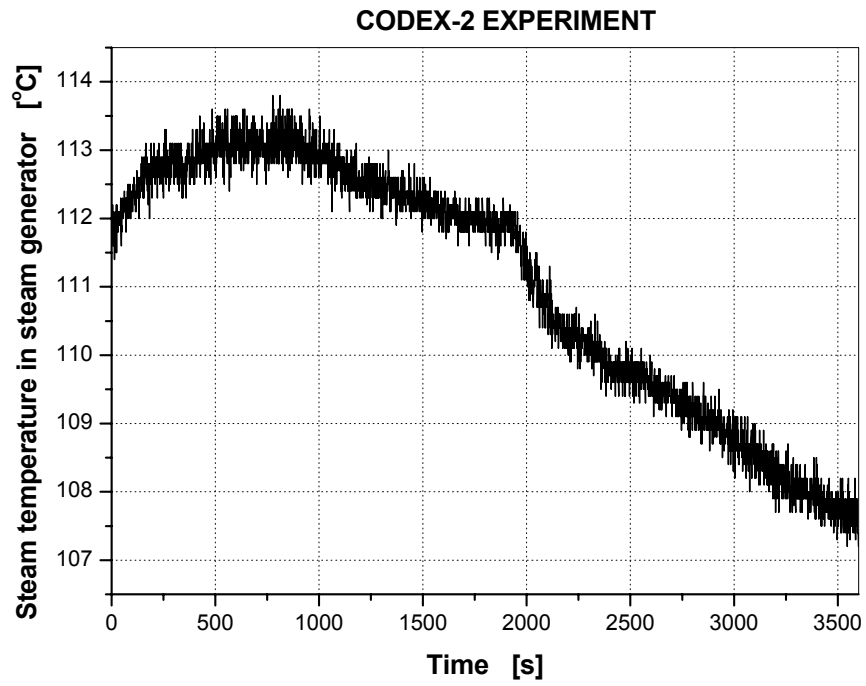


Fig. 21 TSTEAM: steam temperature in steam generator

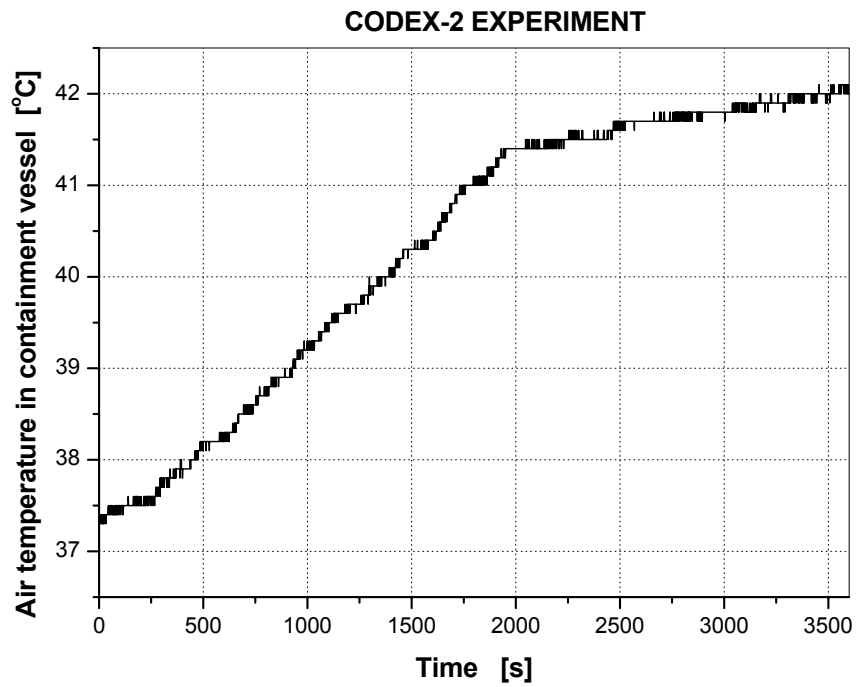


Fig. 22 TAMB: ambient temperature in the containment vessel

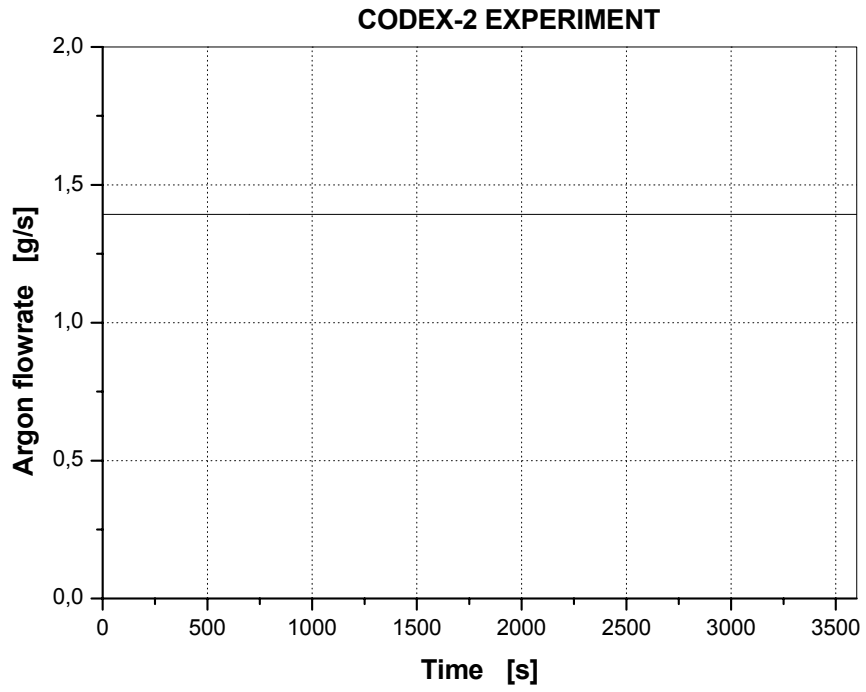


Fig. 23 ARGON: argon flowrate

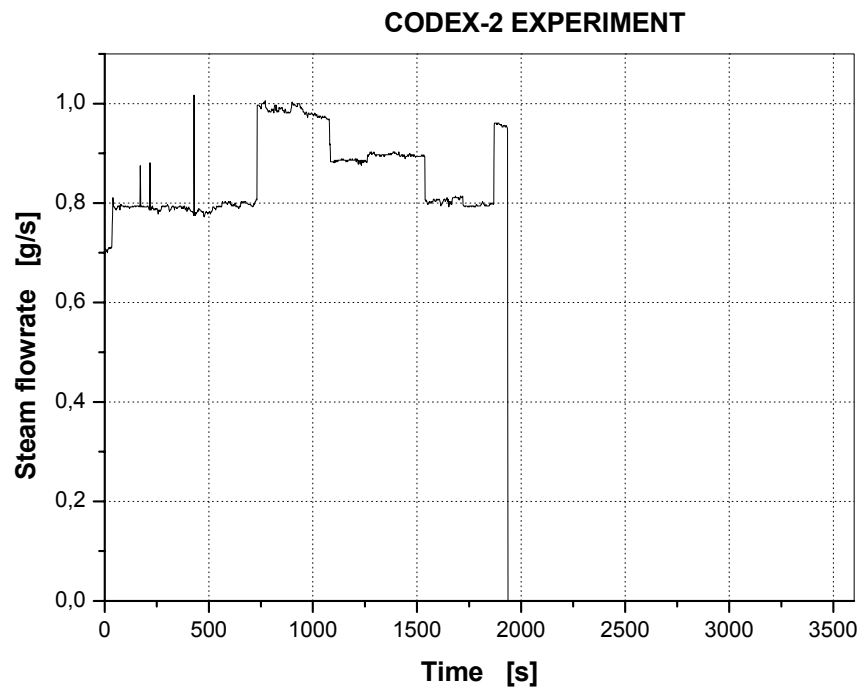


Fig. 24 STEAM: steam flowrate

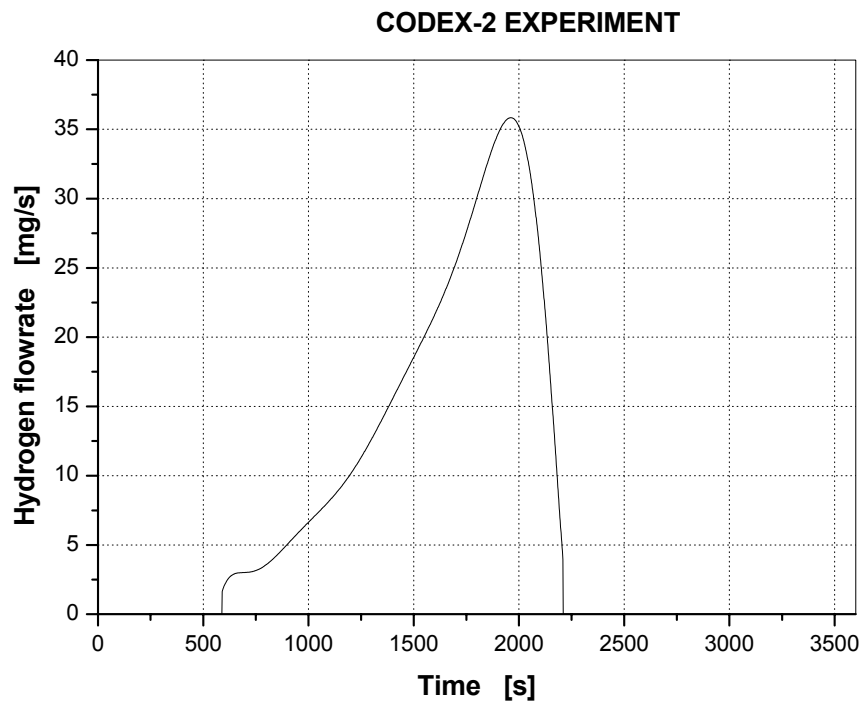


Fig. 25 H2: hydrogen flowrate

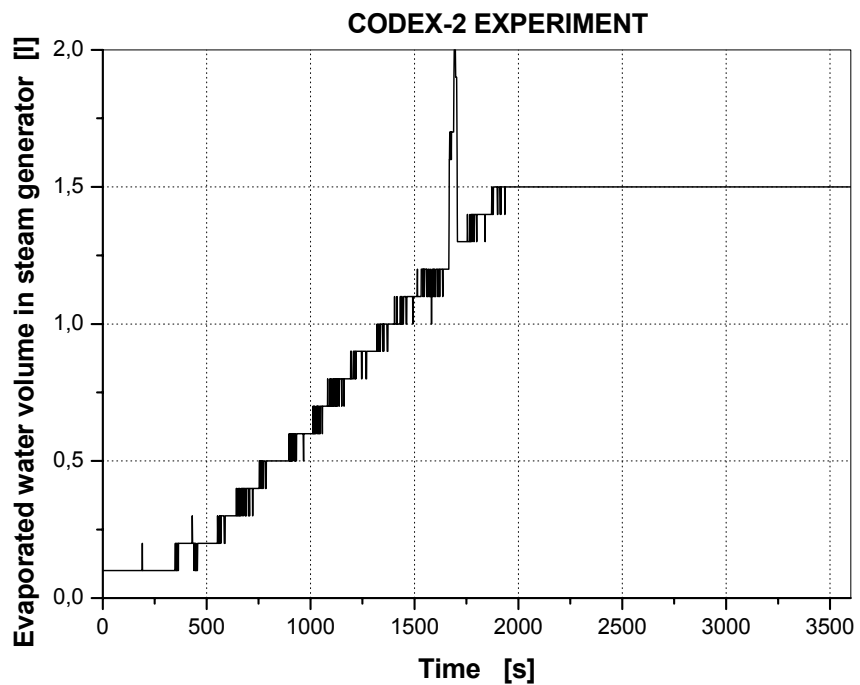


Fig. 26 LSG: evaporated water volume in steam generator (based on water level measurement)

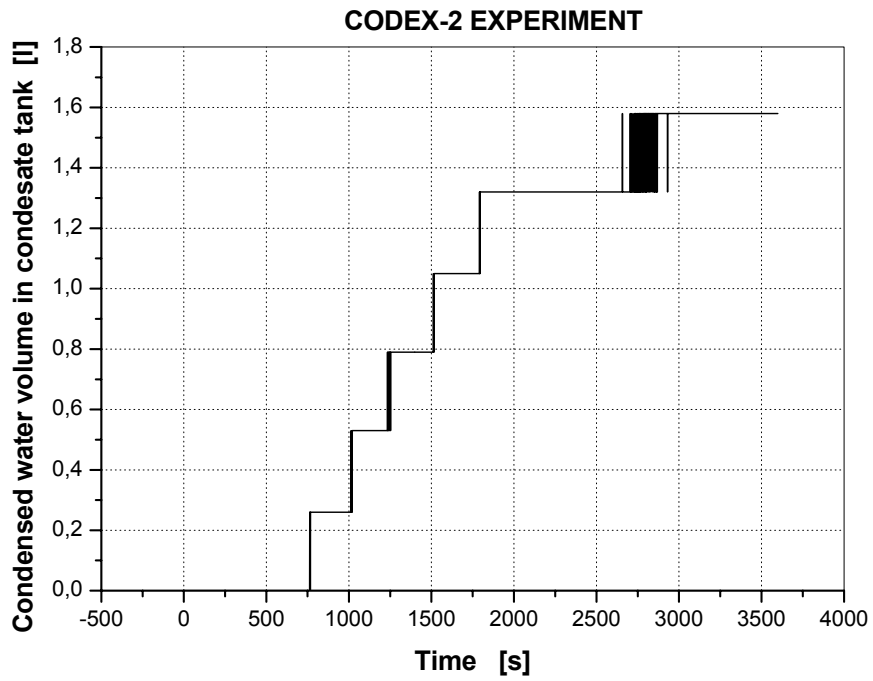


Fig. 27 LCOND: condensed water volume (based on water level measurement)

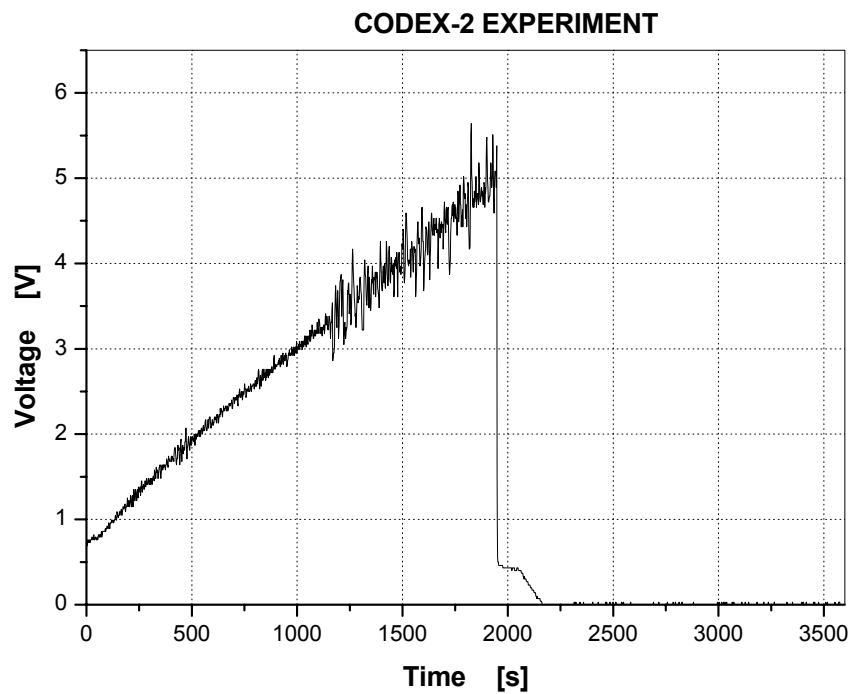


Fig. 28 VOLTAGE: voltage on the heater rods

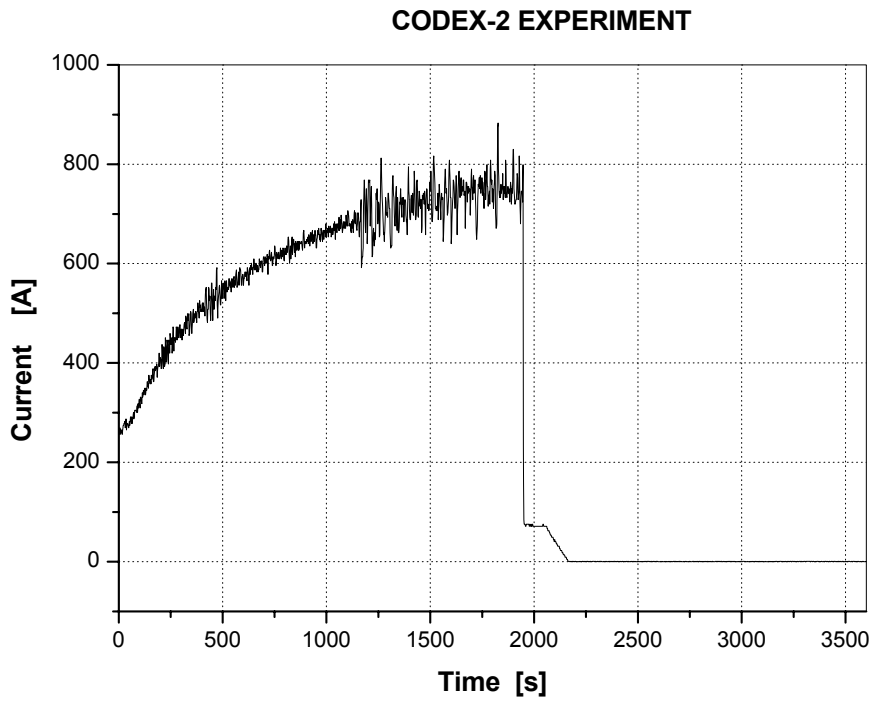


Fig. 29 CURRENT: current on the heater rods

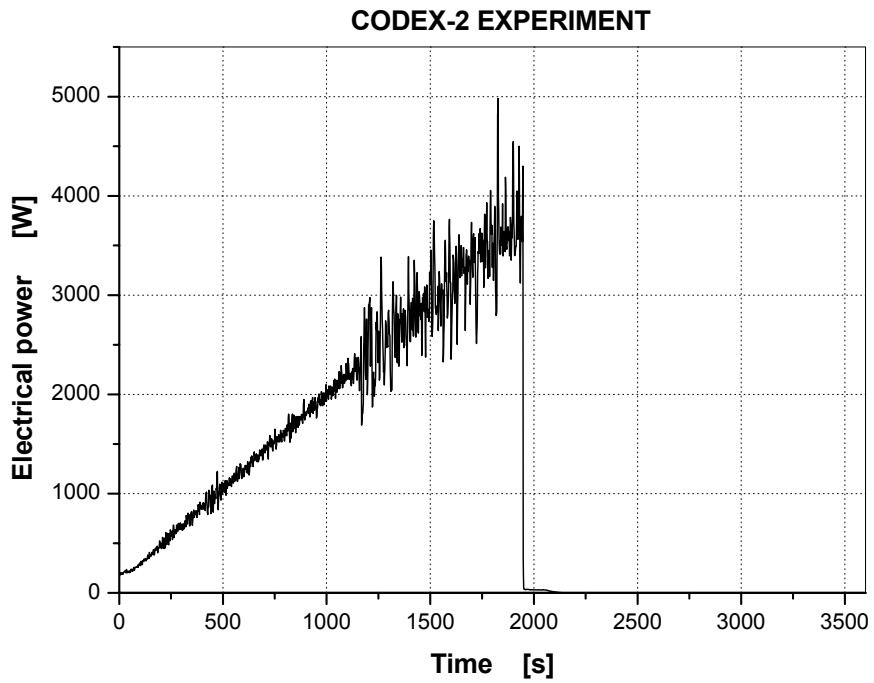


Fig. 30 POWER: total electrical power of the heater rods

CODEX-2 EXPERIMENT

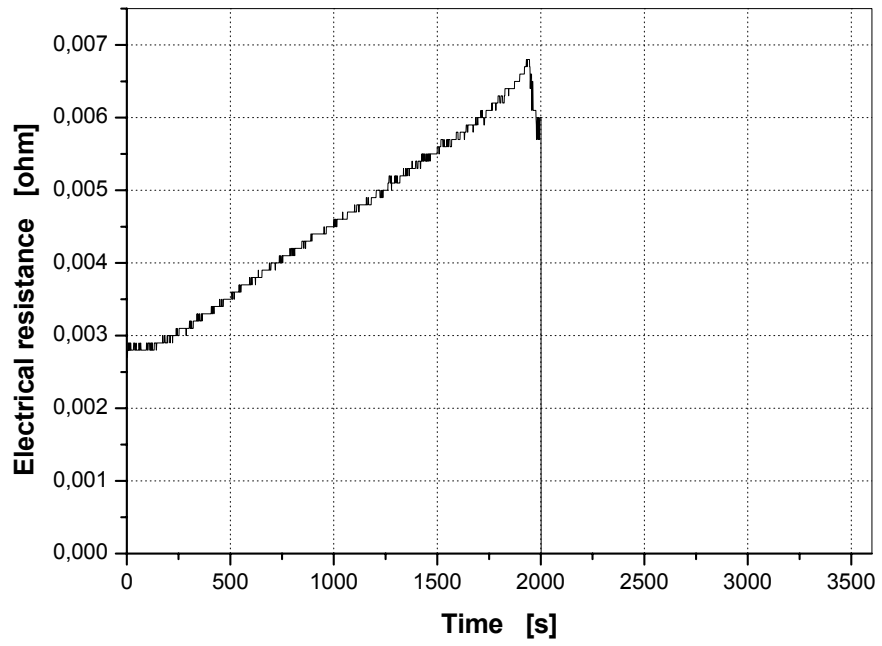


Fig. 31 RESIST: electrical resistance of the heater rods

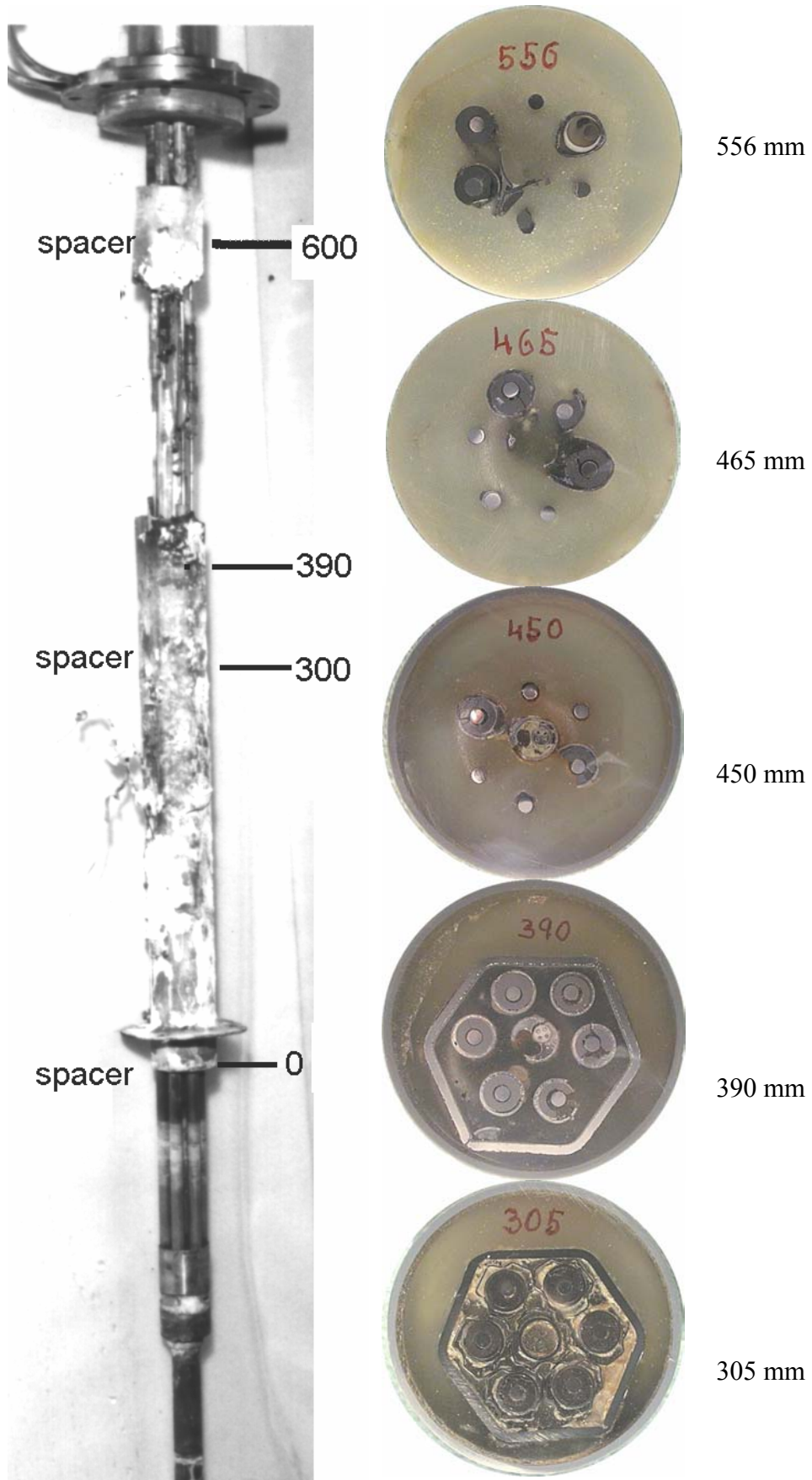


Fig. 32 View and cross sections of the CODEX-2 bundle



Fig. 33 CODEX-2 bundle cross section at 305 mm elevation

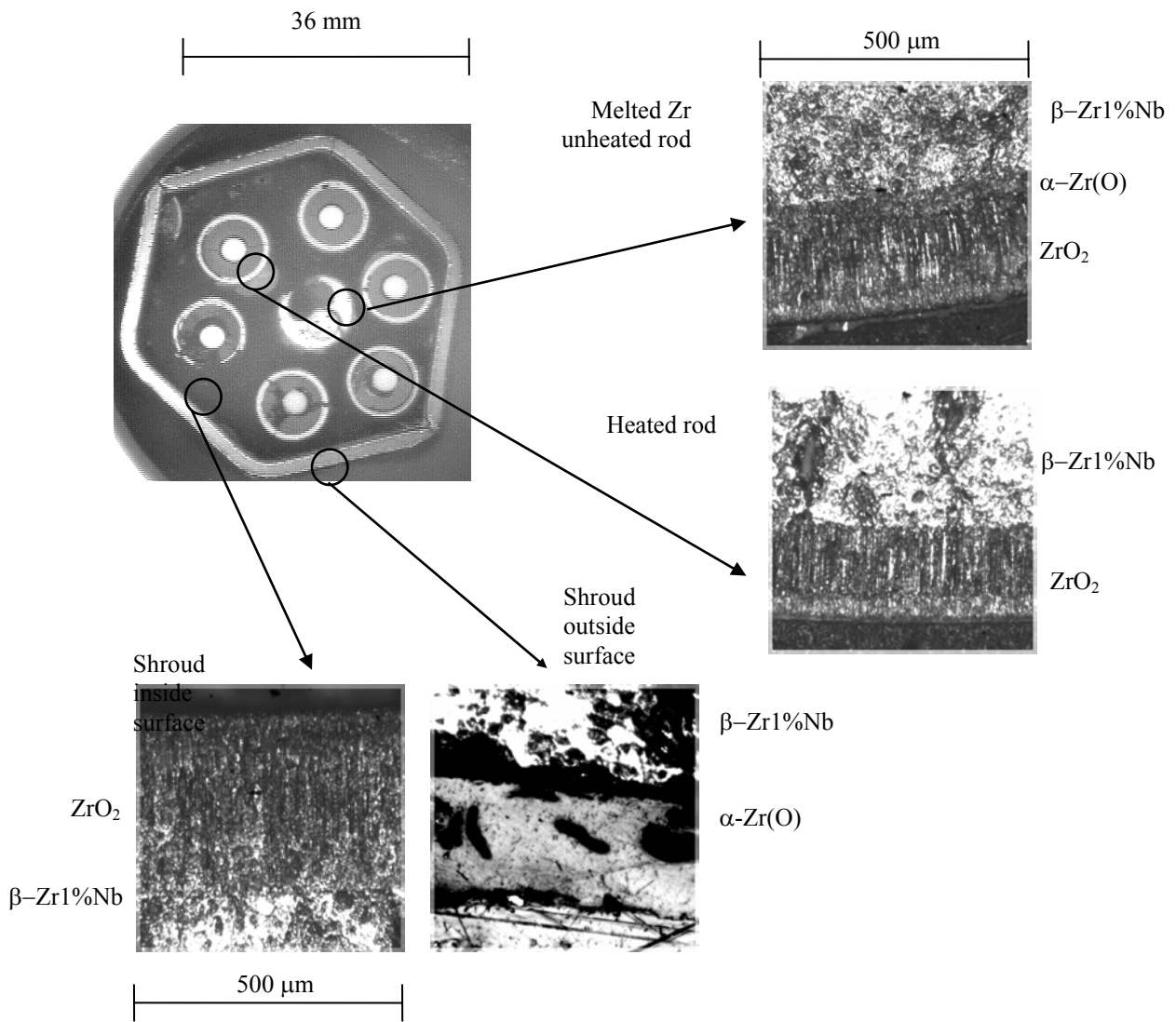


Fig. 34 Horizontal cross-section of CODEX-2 bundle at elevation 390 mm.